Nonlinear Dynamic Analysis of a Thermally Buckled Aircraft Panel using NNMs

Lucas M. Jarman,
Chris VanDamme,
&
Mathew S. Allen,

Department of Engineering Physics
University of Wisconsin
Madison, WI 53706
ljarman@wisc.edu, cvandamme@wisc.edu, msallen@engr.wisc.edu

ABSTRACT
Many thin walled structures experience a combination of static thermal stress and large amplitude dynamic loads. From a dynamic perspective, the heating can change both the linear and nonlinear properties of the system so that completely different responses may be obtained (e.g. they may snap through rather than exhibiting a simple hardening nonlinearity). This work uses the "cold modes" approach to create various reduced order models of one panel from a concept hypersonic vehicle; heating is assumed to change only the linear natural frequencies of the panel, but not the mode shapes or geometrically nonlinear effects. The resulting reduced order models are studied by computing their nonlinear normal modes and their response subject to a random dynamic pressure. The comparisons reveal that much can be inferred about the response from the nonlinear modes.

Keywords: reduced order modeling, geometric nonlinearity, nonlinear normal modes, implicit condensation and expansion, thermal expansion

1. Introduction

Geometric nonlinearity is important for thin plates and shells when deformations approach the thickness of the material, especially when the deformation shape or constraints are such that bending deformation induces membrane stretching, as shown in Fig. 1 for a clamped-clamped beam. If the boundary conditions are rigid and the structure is initially flat, then small changes in temperature can induce significant membrane stresses, changing the behavior significantly. This work has been motivated by the efforts of the United States Air Force (USAF) and the National Aeronautics and Space Administration (NASA) to model and design reusable hypersonic aircraft. At hypersonic speeds (Mach > 5) the aerodynamic pressure is sufficient to cause thin panels to vibrate nonlinearly and thermal loads are also of utmost importance because of the residual stress that they induce and because they can lead to buckling and highly nonlinear vibration of the panel between two buckled states. Similar issues are encountered in stealth aircraft where the engines are buried within the structure to minimize their thermal signature, so that hot exhaust gasses impinge on structural panels.

While the response of a thermally loaded panel could, in principle, be computed using commercial FE codes, the computational cost can measure into the weeks even for relatively simple shell structures with only a few hundred thousand DOF [1]. While much progress has been made in recent years on creating and validating reduced order models (ROM) for geometrically nonlinear structures (e.g. see [2-4] and the review [5]), relatively few works have explored the effect of temperature on the ROM, and on the dynamics of the underlying system. Gordon and Hollkamp [2] created ROMs for a curved panel subjected to a random load and showed how the power spectrum of the response evolved with temperature. They used two approaches, a "cold modes" approach where the linear modes of the structure at room temperature (i.e. no thermal expansion) were used to create the ROM and a "hot modes" approach where the modes at the temperature of interest were used to create the ROM and showed that the two approaches gave almost identical results. Przekop & Rizzi [6] and Spottswood et al [7] also explored the use of reduced order models under thermal loads, and Mignolet et al. have explored various modeling strategies [8-10].

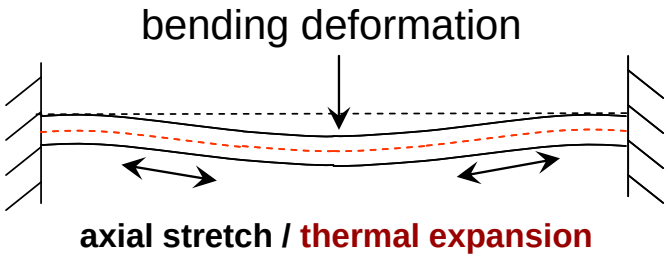

Figure 1. Schematic of clamped-clamped beam subject to bending and thermal loads. When the deformations are small axial stretching can be neglected, but for large deformations the total stiffness increases as the beam must both bend and stretch axially to accommodate the deformation. If the structure is heated then thermal expansion provides additional axial stretching, possibly relaxing the effect due to bending.

This work further explores these issues using a section of the "ramp panel," similar to that which was studied by Culler & McNamara [11]. In order to obtain more insight into the nonlinear dynamic response, the authors employ Nonlinear Modal analysis, using the definition of a Nonlinear Normal Mode (NNM) pioneered by Rosenberg [12] and refined by Vakakis and Kerschen [13, 14]. The ramp panel model is flat, and while it may not have the thermal relief needed for high temperature applications, it does provide an excellent test case since a relatively small temperature change can cause the panel to buckle so that the dynamics change significantly. The linear and nonlinear modal parameters are computed using a "cold modes" reduced order model [7, 15], in which the modes of the room temperature structure are presumed to form an adequate basis for a reduced model. The reduced model is also subjected to random loading and the connection between the nonlinear modes and the random response is explored. The results show that the NNMs give considerable insight into the dynamics. An increase in temperature causes the linear natural frequencies to reduce while leaving the mode shapes largely unchanged. The cold modes approach assumes that the nonlinearity remains unchanged with temperature, and so this reduction in linear stiffness leads to a more strongly nonlinear response and increased interactions between the underlying linear modes.

The paper is outlined as follows. Section 2 briefly reviews the ROM modeling strategy and the definition of nonlinear normal modes used in this work. In Section 3 the methods are applied to the ramp panel using a Titanium material model that includes variation of the modulus and thermal expansion coefficient with temperature. The NNMs and random response are evaluated at various temperatures and conclusions are presented in Section 4.

2. Theoretical Development

After discretization by the finite element method, a nonlinear structure can be represented as,

$$\mathbf{M}\ddot{\mathbf{x}} + \mathbf{K}\mathbf{x} + \mathbf{f}_{NL}(\mathbf{x}) = \mathbf{f}(t) \tag{1}$$

where $\mathbf{M}$ and $\mathbf{K}$ are the $N \times N$ linear mass and stiffness matrices and the geometric nonlinearity exerts a nonlinear restoring force through the $N \times 1$ vector, $\mathbf{f}_{NL}(\mathbf{x})$. External loads are accounted for with the $N \times 1$ vector $\mathbf{f}(t)$, and the $N \times 1$ vectors $\mathbf{x}(t)$ and $\ddot{\mathbf{x}}(t)$ are the displacement and acceleration, respectively.

2.1 Review of Reduced Order Modeling

A reduced order model is obtained by presuming that the response can be well represented using a small set of mode shapes $\left(\mathbf{K} - \omega_r^2 \mathbf{M}\right)\boldsymbol{\varphi}_r = 0$ so that

$$\mathbf{x}(t) = \boldsymbol{\Phi}_m \mathbf{q}(t) \tag{2}$$

Each column in the $N \times m$ mode shape matrix, $\boldsymbol{\Phi}_m$, is a mass normalized mode shape vector, $\boldsymbol{\varphi}$, and $\mathbf{q}(t)$ is a vector of time-dependent modal displacements. The vectors in $\boldsymbol{\Phi}_m$ are truncated to a small set of m mode shapes,

with $m << N$. After applying the modal transformation to the full order Equation (1), the equation of motion for each modal degree of freedom becomes

$$\ddot{q}+\omega_r^2 q_r+\theta_r(q_1,q_2,\ldots q_m)=\boldsymbol{\phi}_r^T \boldsymbol{f}(t) \tag{3}$$

where ω_r is the linear natural frequency, $(\ )^{\mathrm{T}}$ is the transpose operator and q_r is the r^{th} modal displacement. The nonlinearity couples the modal degrees of freedom so the nonlinear modal restoring force is generally a function of all of the modal displacements $\theta_r(\mathbf{q})=\boldsymbol{\varphi}_r^{\mathrm{T}}\mathbf{f}_{NL}(\boldsymbol{\Phi}_m\mathbf{q})$. The response of the modes that are excluded from the modal basis is hoped to be negligible. The theory for geometric nonlinearity reveals that the nonlinear modal restoring force can be modeled with second and third order polynomials, which are shown to be

$$\theta_r(q_1,q_2,\ldots,q_m)=\sum_{i=1}^{m}\sum_{j=i}^{m}B_r(i,j)q_i q_j+\sum_{i=1}^{m}\sum_{j=i}^{m}\sum_{k=j}^{m}A_r(i,j,k)q_i q_j q_k \tag{4}$$

The scalars B_r and A_r are the coefficients of the quadratic and cubic nonlinear stiffness terms, respectively, for the r^{th} equation of motion. The two approaches commonly used to determine these coefficients are the Implicit Condensation and Expansion (ICE) method [16] and the Enforced Displacement (ED) method [1, 17]). In the former, a series of load cases are applied to the model and the resulting displacements are used to form a least squares problem in the nonlinear stiffness coefficients. In the latter, the converse procedure is performed, with displacements enforced on the full order model and constraint forces extracted to solve a set of algebraic equations in B_r and A_r. In some works the ED method has seemed to be more numerically stable, but does not implicitly capture the axial stretching effects, so several axial modes of the structure must be included to obtain accurate results. ICE, on the other hand, requires only dominant bending modes of the structure in the basis, and so the basis tends to be approximately half or one third as large.

2.2 Review of Nonlinear Normal Modes

The nonlinear normal mode definition used throughout this work is based on the definition by Vakakis, Kerschen and others [13, 14], where an NNM is a *not necessarily synchronous periodic solution to the conservative, nonlinear equations of motion*. Nonlinear modes are typically depicted on a frequency versus energy plot, or FEP, which shows how the natural frequency evolves as the response amplitude changes, revealing many qualitative insights into the amplitude dependent dynamics. NNMs are used here to validate the dynamics of NLROMs against those of the original full-order model in a load-independent fashion, as was done in [4].

A pseudo-arclength continuation algorithm, developed originally by Peeters et al. [18], is used throughout this work to compute the NNMs of each of the undamped reduced order models. There exist at least *m* nonlinear normal mode branches that each initiate at a linear mode at low response amplitude. The continuation algorithm uses the shooting technique to find a set of initial conditions and an integration period that satisfy periodicity as the amplitude in the response changes. A shooting function is defined as,

$$\mathbf{H}(T,\mathbf{q}_0,\dot{\mathbf{q}}_0)=\begin{Bmatrix}\mathbf{q}(T,\mathbf{q}_0,\dot{\mathbf{q}}_0)\\ \dot{\mathbf{q}}(T,\mathbf{q}_0,\dot{\mathbf{q}}_0)\end{Bmatrix}-\begin{Bmatrix}\mathbf{q}_0\\ \dot{\mathbf{q}}_0\end{Bmatrix}=\{\mathbf{0}\}, \tag{5}$$

where T is the period of integration, and $\mathbf{q}_0$ and $\dot{\mathbf{q}}_0$ are the initial modal displacements and velocities for a candidate NNM. The NLROM equations must be integrated over a period T subject to the initial conditions; $\mathbf{q}_0$, $\dot{\mathbf{q}}_0$ and T are modified until the magnitude of the shooting function drops below a numerical tolerance and periodicity is satisfied. The NNM solution is then uniquely defined by $\mathbf{q}_0$, $\dot{\mathbf{q}}_0$, and T. These quantities are used by the continuation algorithm to predict a new periodic solution at a slightly different energy level, eventually forming the full locus of NNMs in frequency-energy space.

3. Application to FE of an Aircraft Ramp Panel

The structure modeled was a geometrically nonlinear a ramp panel for a concept hypersonic vehicle. The ramp panel skin is 12 inches (0.3048 m) long, and 10 inches (0.254 m) wide. The skin of the panel has a thickness of 0.065 inches (1.651 mm). Two stiffeners run along the entire length of the skin at the left and right edges. The stiffeners have a depth of 1.25 inches (31.75 mm) and a section thickness of 0.0325 inches (0.8255 mm). The

entire panel is composed of Titanium 6AL-4V, with a Poisson's ratio of 0.31 and temperature dependent elastic modulus and coefficient of thermal expansion shown in Table 1.

Table 1. Elastic modulus and coefficient of thermal expansion for Titanium-6AL-4V at different temperatures [MIL-HDBK-5H, December 1998, pages 5-62 to 5-65].

Temperature (K)	**Elastic Modulus (GPa)**	**Temperature (K)**	**Coef. of Thermal Expansion (K^{-1})**
264.26	110	294.26	8.82×10^{-6}
699.82	82.7	477.59	9.36×10^{-6}
755.37	73.9	810.93	10.3×10^{-6}
810.93	57.4	1144.26	10.3×10^{-6}

The finite element model was created in Abaqus®, meshed with 992 S4RT elements, and is shown in Fig. 2. The model was initially created and analyzed at room temperature (294.26 K), and then the temperature was varied and modal analysis was repeated to understand how the modal properties change as the material properties change with temperature and the pre-stress in the model changes. This was done in Abaqus® by defining a coupled temperature-displacement step, followed by a linear frequency step. Fixed boundary conditions were applied at all edges to prevent bending motion but allow thermal expansion. Specifically, the bottom edges of the stiffeners were constrained in *x* and *z* displacements, but allowed axial extension in the y-direction and rotation. The leading edge of the panel skin was fully constrained in all 6 DOF. The trailing edge of the panel skin was constrained in every DOF except y-displacement.

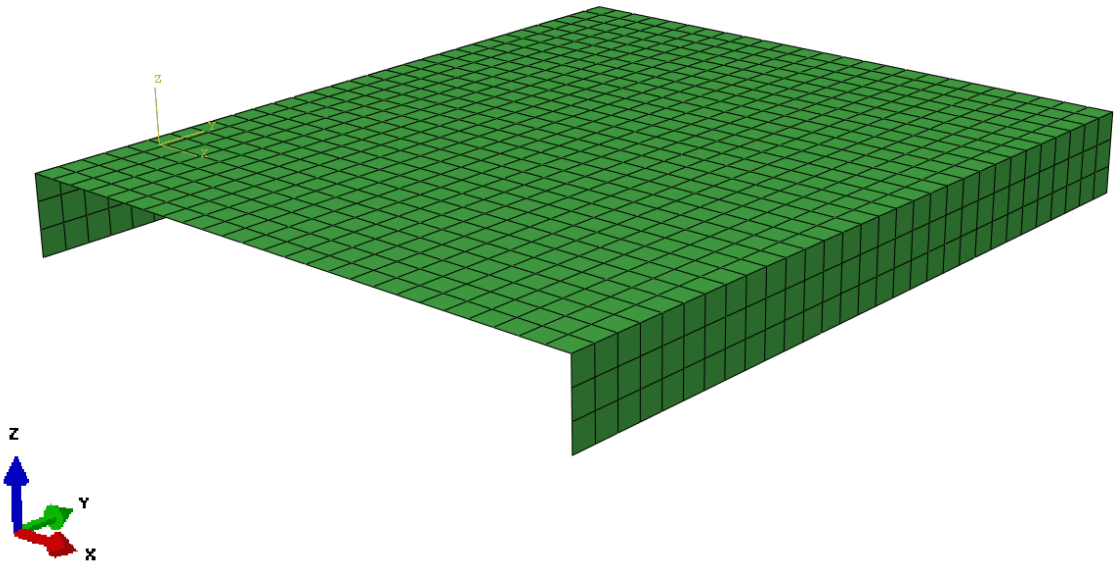

Figure 2. Finite element model of geometrically nonlinear aircraft ramp panel.

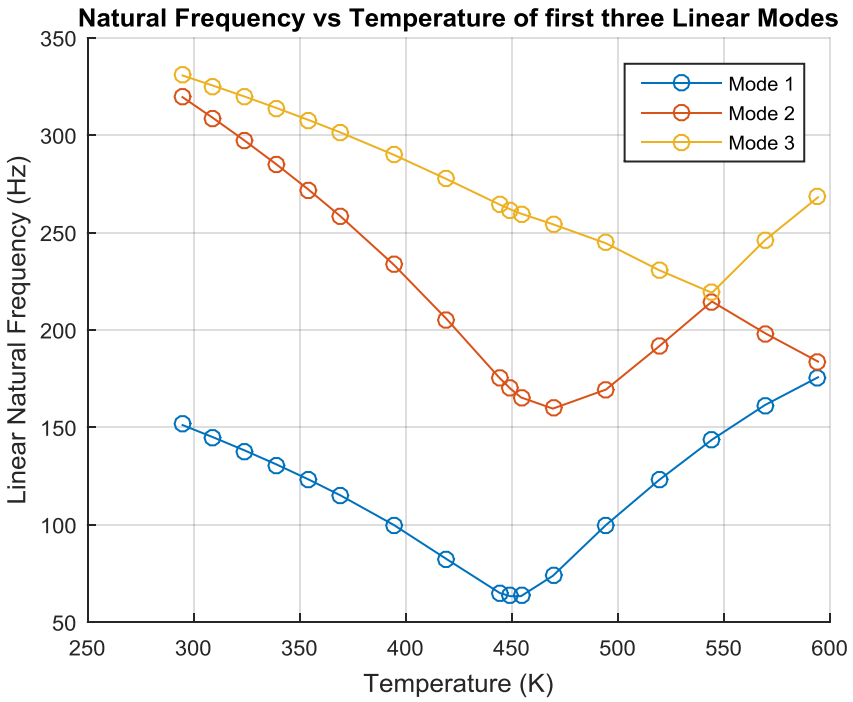

Figure 3. Natural frequencies of the first three linear modes vs. temperature for the panel.

The linear natural frequencies of the first three modes computed at various temperatures using this approach are shown in Fig. 3. All frequencies initially decreased with increasing temperature, but then they each individually reach a point where the frequency begins to increase, presumably as the buckled shape induces enough curvature so that the flat panel becomes arched. Interestingly, the second and third natural frequencies cross at about 545 K. An investigation of the mode shapes, shown in Fig. 4 reveals that the mode shapes switch, so this would need to be accounted for in the cold modes ROM approach.

T = 294.26 K

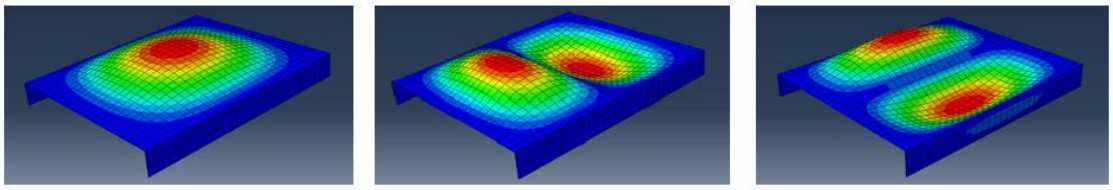

151.39 Hz | 319.86 Hz | 330.85 Hz

T = 475 K

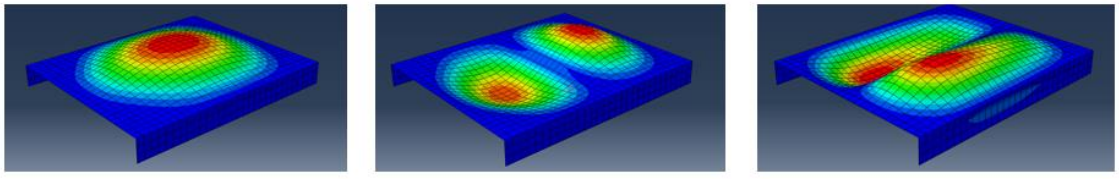

79.778 Hz | 160.2 Hz | 252.34 Hz

T = 540 K

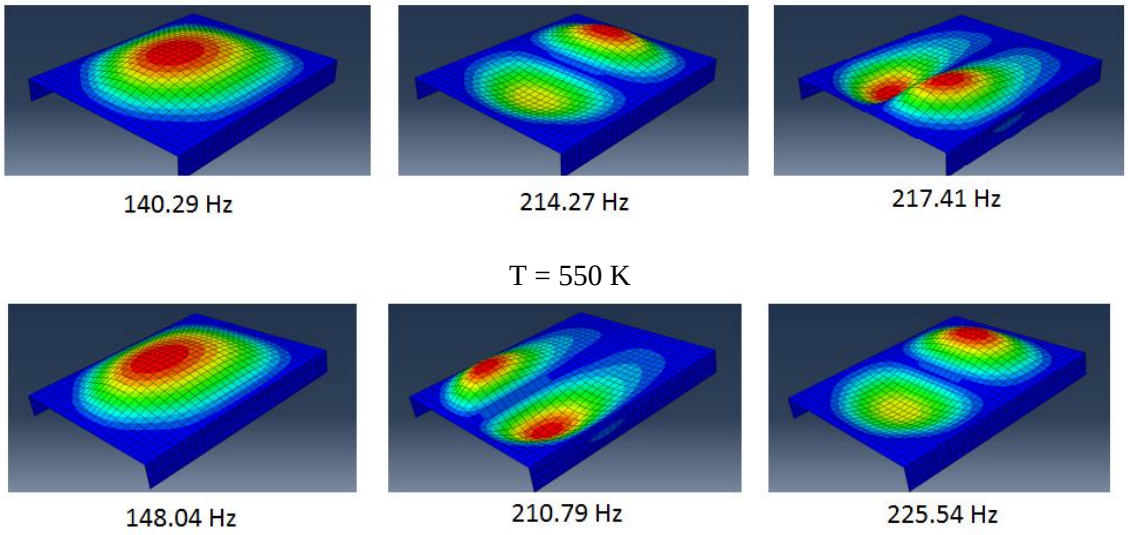

Figure 4. Shapes of the first three linear modes at various temperatures. Note that between 540 K and 550 K, the second and third mode shapes switch order.

The mode shapes shown in Fig. 4 reveal that that, except for the changing order of the modes, the mode shapes seem to remain relatively constant. As a result one would expect the cold modes ROM approach to remain valid.

The ICE method was then used to create a ROM at room temperature. Various combinations of modes were used to generate static load cases, and then static analysis was performed in Abaqus and the resulting force displacement data was used to compute the nonlinear terms in the reduced equations of motion. In all of these cases the load levels were chosen so that the linear structure would deform the average of the skin thickness and stiffener thickness. Fig. 5 shows the FEP of the first NNM for a few candidate ROMs.

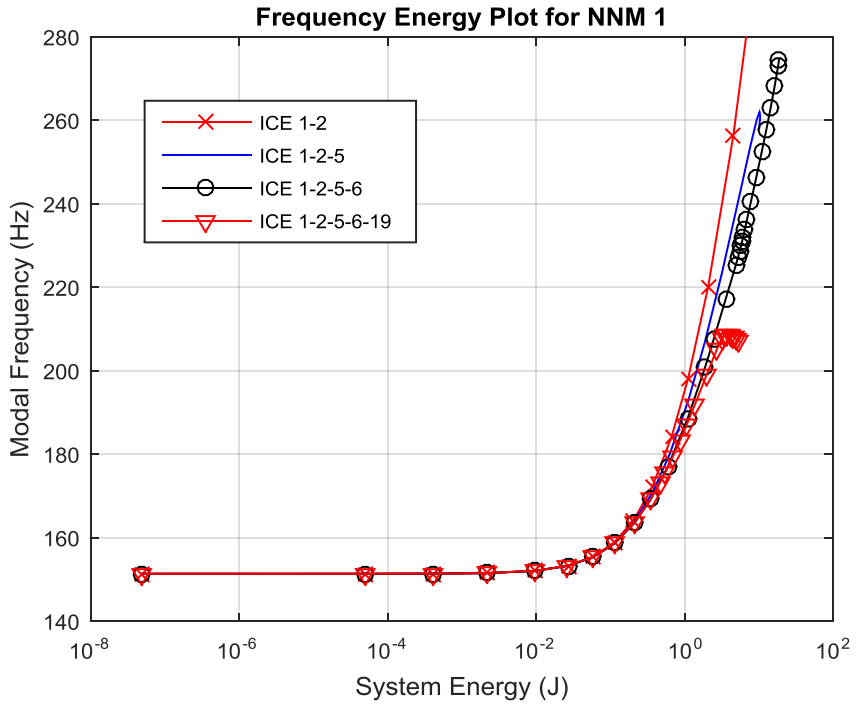

Figure 5. Frequency-Energy Plot of the first Nonlinear Normal Mode of the ramp panel at room temperature for various candidate ROMs.

Initially, a ROM that used only mode 1 was created, and modes were continually added to the basis in the order of their dominance in the static responses used to create the previous ROM. This seemed reasonable since the first NNM was expected to dominate the response and the others were expected to be important only if they were statically coupled to NNM 1. The shapes of the other modes that were added to the ROM are shown in Fig. 6. NNM 1 was found to change very little as higher modes were added to the ROM, however for the five mode ROM the first NNM comes to an internal resonance at 225 Hz and is not able to compute the rest of the backbone. The four mode ROM (containing modes 1, 2, 5 and 6) appeared to agree very well with the five mode ROM (containing modes 1,2,5,6 and 19) and so NNMs were computed at increased temperature for both of these ROMs. As mentioned previously, this was done using a "cold modes" approach [7, 15, 19]. The FEPs for a few temperatures, found using both the four and five mode ROMs, are shown in Fig. 7.

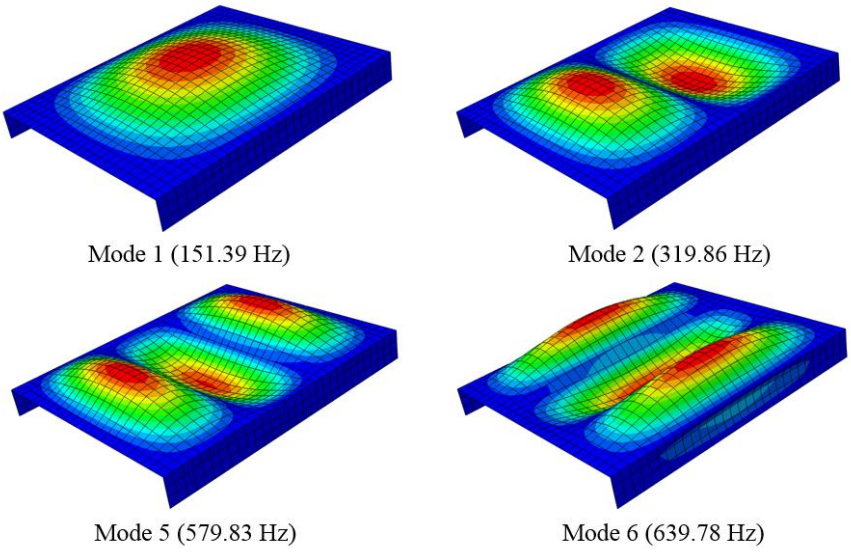

Figure 6. Modes 1,2,5 and 6 used to generate the four mode ROM.

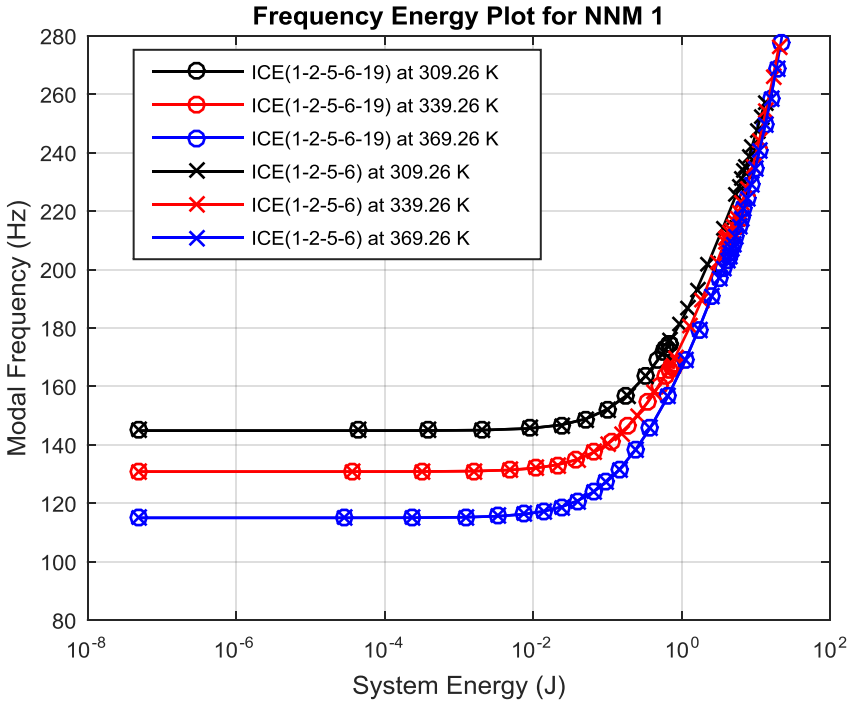

Figure 7. Frequency-Energy Plot of the first NNM for three temperatures, comparing the four and five mode ICE ROMs.

The FEPs for both cases agreed very well, although we were not able to compute the NNM of the five mode ROM to as high of temperatures to internal resonance. Hence, the first NNM from the five mode ROM ran into internal resonance at 170 Hz for the 309.26 K case, 165 Hz for the 339.26 K case, and around 200 Hz for the 369.26 K case. The 369.26 K continuation continued for a while after resonance, but with heavy interaction from other modes affecting reliability of the result. The four mode case ran uninterrupted to at least 260 Hz for all cases, and so it was used from here forward. The FEPs for the four mode ICE 1-2-5-6 ROM are shown in Fig. 8 for a variety of temperatures.

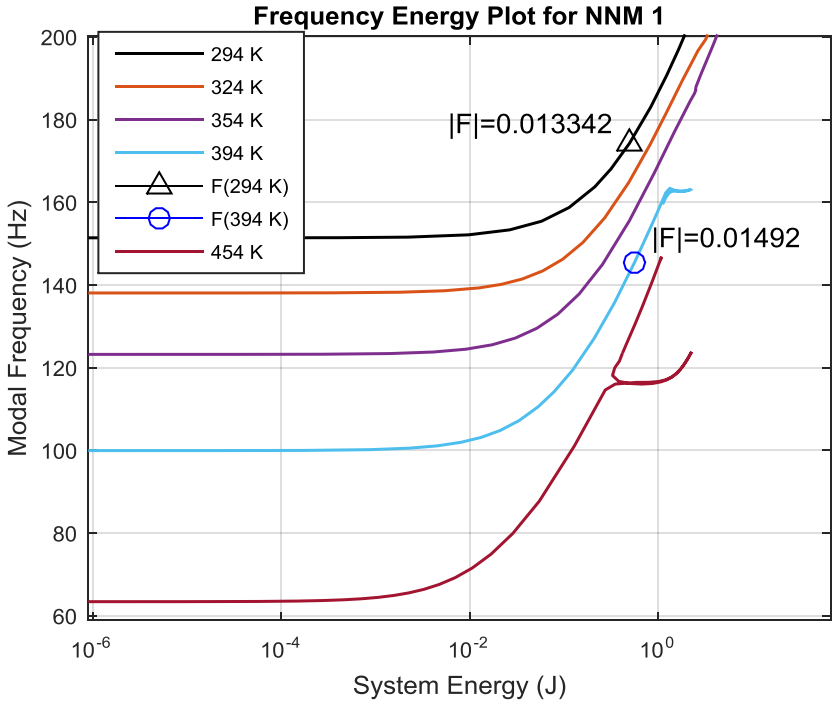

Figure 8. Frequency -Energy Plots for the first NNM of the panel at various temperatures.

The FEP shows that first linear natural frequency of the ROMs decreased with increasing temperature, as expected. However, because the nonlinearity remains the same as the stiffness goes down, the high temperature ROMs also began to diverge from linearity at lower energies. The NNMs at the two higher temperatures were not computed to as high of energies as the others because the algorithm encountered some internal resonance branches and was not able to continue, and the publication schedule of this paper did not allow us to explore this further.

The power balance algorithm in [20, 21] was used to compute how large of a force would be needed to drive the system to various points on the NNM curves. In all cases the force was uniformly distributed in space in the z-direction and sinusoidal at the NNM frequency. The forces computed at 294 K and 394 K, shown in Fig. 8 are nearly the same, and drive the system to almost the same energy, suggesting that the same level of force is needed to drive the system to a certain energy level, even though the linear stiffness has decreased significantly. This suggests that the random response may reach similar levels as the temperature varies, but that the level of nonlinearity excited (as evidenced by the shift or smearing of the resonance frequency) would be much greater at higher temperature. This inference will now be checked by computing the true random response of these NLROMs.

The environment of interest for the panel is a random pressure loading. To evaluate the ROM's performance in this environment, the response of the ROM was found subject to a uniform (over the panel area) pressure that varied randomly in time. The spectrum of the input was white and constant from 0 to 800 Hz, encompassing the first several modes of the panel. The power spectrum of the resulting time response and the power spectral density (PSD) for each case is shown in Fig. 9.

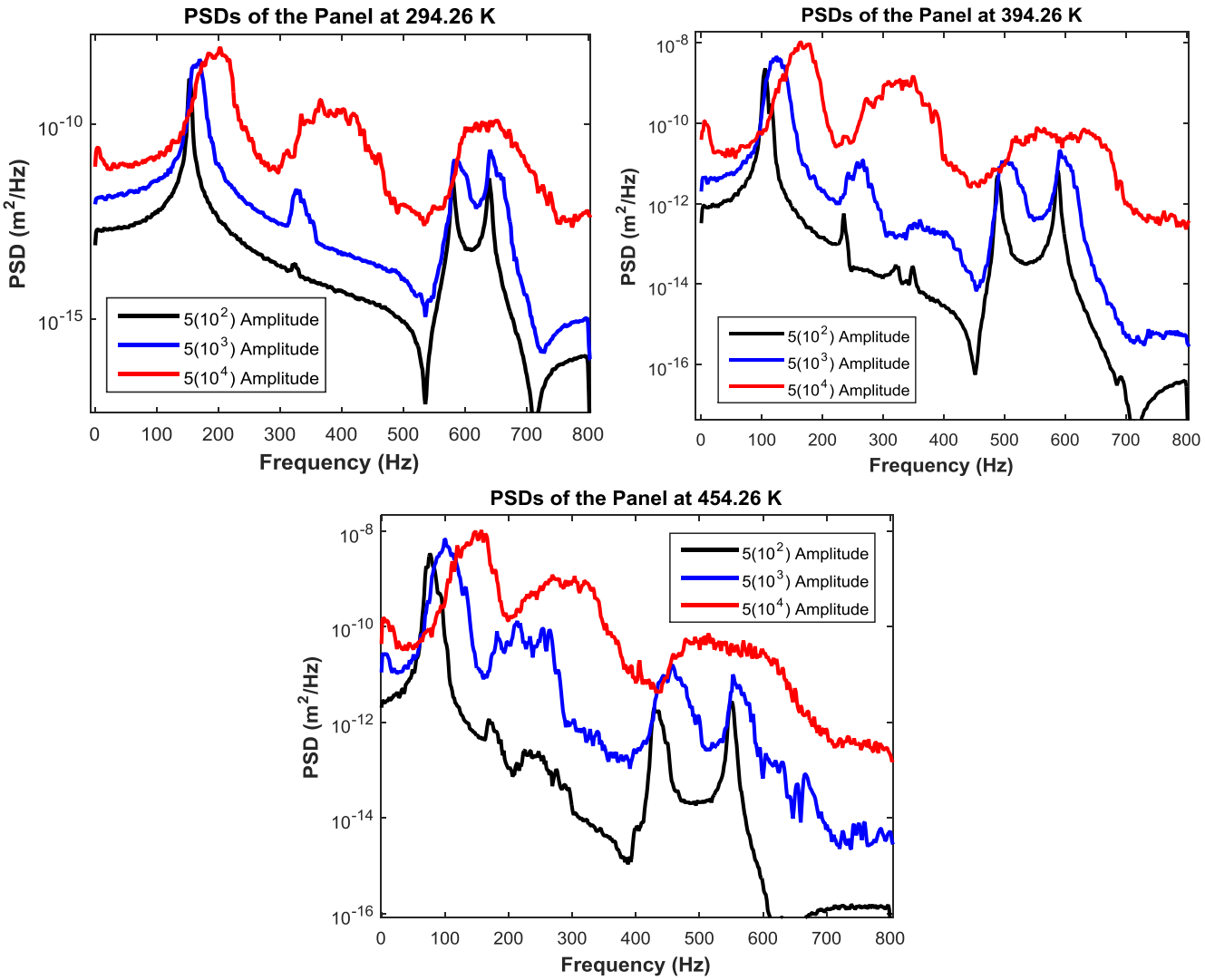

Figure 9. Power Spectral Density at a point near the center of the panel. Each plot shows the panel at three amplitude levels for a different temperature. In each case the pressure was applied in the z-direction on every node on the panel skin with amplitude that varied randomly in time.

Although the nonlinear terms in the EOM were the same in each of these ROMs, the panel's linear stiffness decreased with heating and so it diverged from linearity earlier. Perhaps most revealing of the PSDs is the first, and lowest amplitude case shown in Fig. 9. In this case the room temperature ROM still looks very linear and has a peak corresponding to the first linear frequency. For the same amplitude the 394 K ROM underwent a frequency shift of about 5 Hz, and the 454 K ROM experienced a shift of 10 Hz, corresponding to a point far up the frequency-energy curve for that temperature. Increasing the amplitude of the pressure made the responses all nonlinear. For reference, at 294 K the RMS displacement at the center of the panel was 0.09, 0.27 and 0.57 mm at the three load levels, while at 454 K it increased to 0.2, 0.4 and 0.7 mm. Clearly the nonlinearity sets in at lower amplitudes as the temperature increased, just as one would have expected based on the NNMs. It is also interesting to note that the RMS displacement increased by only about a factor of two for every order of magnitude increase in the pressure amplitude. This highlights the value in exploiting nonlinearity in a design such as this.

The modal interactions are also evident in the PSDs; these can be seen more clearly in modal coordinates. Shown in Fig. 10 is the PSD of Modes 1 and 2 at the intermediate amplitude. As the temperature increases and the

response becomes more nonlinear, mode 2 is more strongly excited. Mode 2 would not be excited in a linear response due to its anti-symmetric shape, so presumably it is excited due to an interaction with Mode 1.

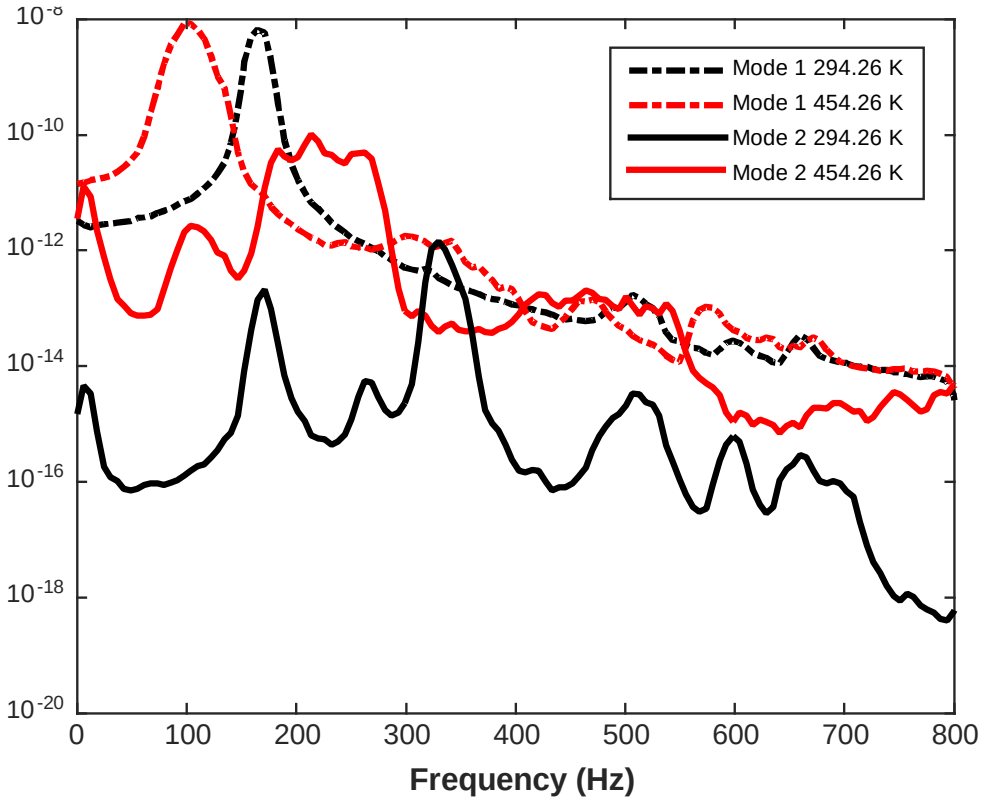

Figure 10. Power Spectral Density of linear modal amplitudes of modes 1 and 2 at room temperature, and 454.26 K for a forcing amplitude of 5×10^3 (the intermediate forcing case).

4. Conclusions

This work investigated an approach to generate reduced order models for dynamic analysis of a structure that experiences thermal deformation. The ROMs enabled us to compute the nonlinear frequency-energy dependence and dynamic response of the heated FE model at a dramatically lower computational cost than would have been required on the full order model. The temperature dependence of the behavior of a ramp panel was clearly revealed. Temperature was shown to have a significant effect on the dynamics of the system. As the panel was heated it became more compliant due to residual stress, and this caused the linear natural frequencies to decrease while the nonlinearity in the model (for the cold modes approach) remained unchanged. This increased compliance caused the system to behave more nonlinearly for the same forcing amplitude, leading to smearing of the resonance in the PSD and enhanced modal interactions.

5. Future Work

A few things are notably absent from this paper due to the tight publication schedule. First, the ROMs have not been validated other than checking that they converge as modes are added to the basis. Perhaps we could argue that this mimics a realistic case in which a model is too large to compute the truth NNMs. However, even with a large model we expect that it would be possible to at least peform a periodicity check by integrating the full FEM with the initial condition from the ROM, as done in [22]. It would also be useful to validate the PSDs that were obtained using the ROM by integrating the full order model. However, even with this simple model it took about one day to complete full order time integration over a long enough window to allow the PSD to be computed, and so in the time that was required to perform all of the analyses here it was not possible to finish debugging even one integration of the full order Abaqus model. Finally, the cold modes approach does make a significant

assumption about the modal basis of the ROM, and for the large displacements observed here it would seem wise to also explore the "hot modes" approach. This will certainly be pursued in future works.

Acknowledgements
The authors wish to thank Joseph D. Schoneman from ATA Engineering, Huntsville, AL for providing the impetus for the work and for help implementing the thermal models and Dr. Joseph Hollkamp from the Structural Sciences Center at the Air Force Research Laboratory for helpful suggestions and discussions regarding the ROM modeling.

References

[1] *R. Perez, X. Q. Wang, and M. P. Mignolet, "Nonintrusive structural dynamic reduced order modeling for large deformations: Enhancements for complex structures,"* Journal of Computational and Nonlinear Dynamics, *vol. 9, 2014.*

[2] *R. W. Gordon and J. J. Hollkamp, "Reduced-Order Models for Acoustic Response Prediction," AFRL-RB-WP-TR-2011-3040, Jul. 2011.*

[3] *J. J. Hollkamp, R. W. Gordon, and S. M. Spottswood, "Nonlinear modal models for sonic fatigue response prediction: a comparison of methods,"* Journal of Sound and Vibration, *vol. 284, pp. 1145-63, 2005.*

[4] *R. J. Kuether, B. Deaner, M. S. Allen, and J. J. Hollkamp, "Evaluation of Geometrically Nonlinear Reduced Order Models with Nonlinear Normal Modes "* AIAA Journal, *vol. 53, pp. 3273-3285, 2015.*

[5] *M. P. Mignolet, A. Przekop, S. A. Rizzi, and S. M. Spottswood, "A review of indirect/non-intrusive reduced order modeling of nonlinear geometric structures,"* Journal of Sound and Vibration, *vol. 332, pp. 2437-2460, 2013.*

[6] *A. Przekop and S. A. Rizzi, "Dynamic snap-through of thin-walled structures by a reduced-order method,"* AIAA Journal, *vol. 45, pp. 2510-2519, 2007.*

[7] *S. M. Spottswood, J. J. Hollkamp, and T. G. Eason, "Reduced-order models for a shallow curved beam under combined loading,"* AIAA Journal, *vol. 48, pp. 47-55, 2010.*

[8] *M. Matney, R. A. Perez, S. M. Spottswood, X. Q. Wang, and A. M. P. Mignolet, "Nonlinear structural reduced order modeling methods for hypersonic structures," in* 53rd AIAA/ASME/ASCE/AHS/ASC Structures, Structural Dynamics and Materials Conference, April 23, 2012 - April 26, 2012*, Honolulu, HI, United states, 2012.*

[9] *A. G. Radu, B. Yang, K. Kim, and M. P. Mignolet, "Prediction of the dynamic response and fatigue life of panels subjected to thermo-acoustic loading," in* Collect. of Pap. - 45th AIAA/ASME/ASCE/AHS/ASC Struct., Struct. Dyn. and Mater. Conf.; 12th AIAA/ASME/AHS Adapt. Struct. Conf.; 6th AIAA Non-Deterministic Approaches Forum; 5th AIAA Gossamer Spacecraft Forum, April 19, 2004 - April 22, 2004, *Palm Springs, CA, United states, 2004, pp. 520-528.*

[10] *K. Kim, B. Yang, M. P. Mignolet, and S. M. Spottswood, "Fatigue life prediction of panels subjected to thermo-acoustic loading," in* 44th AIAA/ASME/ASCE/AHS/ASC Structures, Structural Dynamics, and Materials Conference, April 7, 2003 - April 10, 2003, *Norfolk, VA, United states, 2003, pp. 3430-3438.*

[11] *A. J. Culler and J. J. McNamara, "Coupled Flow-Thermal-Structural Analysis for Response Prediction of Hypersonic Vehicle Skin Panels," presented at the 51st AIAA/ASME/ASCE/AHS/ASC Structures, Structural Dynamics, and Materials Conference, Orlando, Florida, 2010.*

[12] *R. M. Rosenberg, "Normal modes of nonlinear dual-mode systems,"* Journal of Applied Mechanics, *vol. 27, pp. 263–268, 1960.*

[13] *A. F. Vakakis, "Non-linear normal modes (NNMs) and their applications in vibration theory: an overview,"* Mechanical Systems and Signal Processing, *vol. 11, pp. 3-22, 1997.*

[14] *G. Kerschen, M. Peeters, J. C. Golinval, and A. F. Vakakis, "Nonlinear normal modes. Part I. A useful framework for the structural dynamicist,"* Mechanical Systems and Signal Processing, *vol. 23, pp. 170-94, 2009.*

[15] *R. W. Gordon and J. J. Hollkamp, "Reduced-order Models for Acoustic Response Prediction," Air Force Research Laboratory, AFRL-RB-WP-TR-2011-3040, Dayton, OH2011.*

[16] *J. J. Hollkamp and R. W. Gordon, "Reduced-order models for nonlinear response prediction: Implicit condensation and expansion,"* Journal of Sound and Vibration, *vol. 318, pp. 1139-1153, 2008.*

[17] *A. A. Muravyov and S. A. Rizzi, "Determination of nonlinear stiffness with application to random vibration of geometrically nonlinear structures,"* Computers and Structures, *vol. 81, pp. 1513-1523, 2003.*

[18] *M. Peeters, R. Viguie, G. Serandour, G. Kerschen, and J. C. Golinval, "Nonlinear normal modes, part II: toward a practical computation using numerical continuation techniques,"* Mechanical Systems and Signal Processing*, vol. 23, pp. 195-216, 2009.*

[19] *A. Przekop, M. A. Stover, and S. A. Rizzi, "Nonlinear reduced-order simulation using stress-free and pre-stressed modal bases," in* 50th AIAA/ASME/ASCE/AHS/ASC Structures, Structural Dynamics and Materials Conference, May 4, 2009 - May 7, 2009*, Palm Springs, CA, United states, 2009.*

[20] *R. J. Kuether, L. Renson, T. Detroux, C. Grappasonni, G. Kerschen, and M. S. Allen, "Nonlinear Normal Modes, Modal Interactions and Isolated Resonance Curves,"* Journal of Sound and Vibration*, vol. 351, 2015.*

[21] *T. L. Hill, A. Cammarano, S. A. Neild, and D. J. Wagg, "Interpreting the forced responses of a two-degree-of-freedom nonlinear oscillator using backbone curves,"* Journal of Sound and Vibration*, vol. 349, pp. 276-288, 2015.*

[22] *R. J. Kuether and M. S. Allen, "Validation of Nonlinear Reduced Order Models with Time Integration Targeted at Nonlinear Normal Modes," presented at the 33rd International Modal Analysis Conference (IMAC XXXIII), Orlando, Florida, 2015.*